

MPAD: A New Dimension-Reduction Method for Preserving Nearest Neighbors in High-Dimensional Vector Search

Jiuzhou Fu
University of Washington
jiuzhou@uw.edu

Dongfang Zhao
University of Washington
dzhao@cs.washington.edu

ABSTRACT

High-dimensional vector embeddings are widely used in retrieval systems, yet dimensionality reduction (DR) is seldom applied due to its tendency to distort nearest-neighbor (NN) structure critical for search. Existing DR techniques such as PCA and UMAP optimize global or manifold-preserving criteria, rather than retrieval-specific objectives. We present **MPAD**—Maximum Pairwise Absolute Difference, an unsupervised DR method that explicitly preserves approximate NN relations by maximizing the margin between k -NNs and non- k -NNs under a soft orthogonality constraint. This design enables MPAD to retain ANN-relevant geometry without supervision or changes to the original embedding model. Experiments across multiple domains show that MPAD consistently outperforms standard DR methods in preserving neighborhood structure, enabling more accurate search in reduced dimensions.

1 INTRODUCTION

1.1 Background and Motivation

Vector embeddings are foundational to modern retrieval systems, underpinning applications in language models, image retrieval, and recommendation. These embeddings typically live in high-dimensional spaces (e.g., 768 or 1024 dimensions), where similarity is computed via Euclidean or cosine distance. However, operating in such high-dimensional spaces presents several challenges: (i) nearest-neighbor search becomes computationally expensive; (ii) storage overhead grows linearly with dimensionality; and (iii) due to the curse of dimensionality, distances tend to concentrate, making it harder to distinguish truly similar items from dissimilar ones. These issues motivate the need for effective dimensionality reduction (DR) to compress embeddings without sacrificing retrieval performance.

While classical DR techniques like Principal Component Analysis (PCA) [24], t-SNE [46], and UMAP [35] offer ways to project high-dimensional data into lower dimensions, they are not designed with nearest neighbors in mind. These methods prioritize global variance, local manifold continuity, or visualization quality—objectives that do not align with preserving nearest-neighbor (NN) structure crucial for vector search. As a result, when used in retrieval pipelines, they often degrade search accuracy by distorting the fine-grained geometry around each point. This disconnect has discouraged the use of DR in vector databases, despite its potential benefits in efficiency and scalability.

This gap between the potential of dimensionality reduction and its practical limitations in search motivates the need for neighborhood-aware DR methods. Ideally, such a method should preserve the relative similarity between a point and its true k -nearest neighbors (k -NNs), even after projection into a low-dimensional space. Moreover, the method should be compatible with precomputed

embeddings, operate in an unsupervised setting, and avoid retraining or model-specific dependencies. While some supervised techniques attempt to enforce neighborhood structure using labeled data or contrastive objectives, they are not applicable in general-purpose retrieval where labeled neighbors are unavailable. Thus, an unsupervised, geometry-sensitive DR technique that aligns with approximate nearest neighbor (ANN) principles remains largely missing.

Our work addresses this need by proposing a retrieval-centric DR method that aligns directly with the structure of ANN queries. Rather than preserving global distance metrics, our goal is to preserve relative neighborhood rankings—namely, ensuring that true k -nearest neighbors remain closer than non-neighbors after projection. This shift in objective calls for a fundamentally different formulation than traditional DR methods, and forms the core motivation for our proposed solution.

1.2 Proposed Work

To bridge the gap between practical efficiency and semantic fidelity in multi-vector retrieval, we propose a new dimensionality reduction framework called **MPAD** (Maximum Pairwise Absolute Difference). Unlike traditional DR techniques that aim to preserve global variance or pairwise distances, MPAD explicitly targets *approximate nearest neighbor (ANN)* fidelity. It formulates an unsupervised optimization objective that prioritizes the relative ordering of each vector’s true k -nearest neighbors over its non-neighbors in the low-dimensional space. By encouraging margin-based separation between neighbors and distractors, MPAD ensures that ANN-sensitive geometry is preserved during projection.

From a system design perspective, MPAD is lightweight and deployment-friendly. It does not require access to the original embedding model or labeled training data. Instead, it operates directly on a given high-dimensional dataset and produces a projection matrix that can be applied to new data without retraining. To avoid collapsed or degenerate projections, MPAD incorporates a soft orthogonality constraint, ensuring that the projected space remains expressive and well-structured. This makes MPAD compatible with a broad class of pre-trained encoders and easily integrable into existing vector search pipelines as a post-processing step.

Beyond empirical improvements, MPAD enjoys favorable geometric and theoretical properties. We show that it preserves topological neighborhood information under affine transformations such as translation and rotation. For non-uniform scaling, we introduce a novel condition-number-based bound that quantifies how distortion accumulates during projection. This allows us to formally characterize the approximation stability of MPAD—a property that is rarely analyzed in prior DR literature. Together, these properties

establish MPAD not only as a practical DR tool for ANN but also as a theoretically grounded algorithm.

1.3 Contributions

This paper makes the following key contributions:

- We propose **MPAD**, a new unsupervised dimensionality reduction method designed specifically for preserving nearest-neighbor structure in approximate vector search, contrasting with traditional DR techniques that focus on global geometry or visualization.
- We provide a rigorous theoretical analysis of MPAD, including its robustness under geometric transformations and a novel condition-number-based bound under non-uniform scaling.
- We empirically evaluate MPAD across multiple real-world datasets, including text and image embeddings, and show that it consistently outperforms standard DR baselines (e.g., PCA, UMAP, random projections) in maintaining top- k neighbor recall in the reduced space.

In the remainder of this paper, we systematically develop and evaluate our proposed dimensionality reduction framework. Section 2 reviews classical and modern dimensionality reduction techniques, with emphasis on their limitations in preserving local neighborhood structures for approximate nearest neighbor (ANN) tasks. Section 3 introduces the *Metric-Preserving Asymmetric Dimensionality reduction* (MPAD) method, including its notation, algorithmic formulation, theoretical foundations, and computational analysis. In Section 4, we conduct extensive empirical evaluations of MPAD against state-of-the-art baselines across diverse datasets, examining both accuracy and robustness under varying parameters. Finally, Section 5 surveys additional literature in manifold learning, high-dimensional indexing, and neighbor-preserving reduction, situating our work within broader research trends, and Section 6 concludes with a discussion of future directions.

2 PRELIMINARIES OF DIMENSIONALITY REDUCTION

Dimensionality reduction (DR) is a long-standing challenge in machine learning, statistics, and data management [23, 28, 47]. A wide range of methods have been proposed to reduce the dimensionality of data while attempting to preserve its structure. However, few existing DR techniques explicitly focus on preserving local neighborhood information, especially in the context of approximate nearest neighbor (ANN) search [3, 5, 22, 37]. This section categorizes and reviews key DR methods, their relationship to ANN preservation, and related advances in neighbor-aware dimensionality reduction.

2.1 Principal Component Analysis (PCA)

[2, 24] remains one of the most foundational and widely-used linear dimensionality reduction (DR) techniques across scientific and engineering domains. PCA seeks a set of orthogonal directions—known as principal components—along which the data exhibits maximum variance. By projecting high-dimensional data onto a subspace spanned by the top m principal components, PCA provides a compact representation that retains as much of the data’s

global structure as possible. Its solution is closed-form and can be efficiently computed via singular value decomposition (SVD), making it particularly appealing for large-scale datasets where both accuracy and computational tractability are important.

Despite its widespread use, PCA is inherently a global method: it optimizes for directions that explain the largest variance across the entire dataset, without regard to local geometry or neighborhood preservation. This characteristic makes PCA ill-suited for tasks that rely on maintaining k -nearest neighbor (k -NN) relations—such as approximate nearest neighbor (ANN) search and information retrieval—since small distances between semantically similar points can be distorted during projection. In such contexts, preserving local topology is often more important than capturing dominant global trends, which PCA overlooks.

Over the years, numerous variants and generalizations of PCA have been proposed to address its limitations or adapt it to specific settings. For instance, *Sparse PCA* [53] imposes sparsity constraints on the principal components to improve interpretability and variable selection. *Principal Curves* [20] extend PCA by fitting smooth one-dimensional curves that pass through the middle of the data, capturing non-linear structure. *Multilinear PCA (MPCA)* [30] adapts PCA to tensor-valued data by preserving multi-way structure. *Refined PCA* [43] improves projection quality by iteratively updating principal directions, and *Robust PCA* [9] decomposes data into low-rank and sparse components to resist outliers. Kernel PCA, discussed separately, is a further extension to non-linear settings via kernel methods.

2.2 Kernel PCA

[33, 42] extends the classical Principal Component Analysis (PCA) by first mapping the input data into a high-dimensional feature space via a non-linear kernel function, and then performing linear PCA in that transformed space. This approach enables the discovery of non-linear patterns and manifold structures in the original data that standard PCA—restricted to linear projections—cannot capture. Commonly used kernels include the Gaussian (RBF) and polynomial kernels, which introduce flexibility in modeling complex geometric relationships between data points.

However, this expressiveness comes at a substantial computational cost. Kernel PCA requires constructing an $N \times N$ kernel matrix—where N is the number of samples—and computing its eigenvalue decomposition, resulting in a time complexity of $O(N^3)$ and space complexity of $O(N^2)$. These scaling limitations make Kernel PCA impractical for large-scale or streaming datasets, particularly in applications such as approximate nearest neighbor (ANN) search, where efficiency is critical. Moreover, the implicit mapping complicates downstream interpretability and integration into vector database systems that favor explicit linear transformations.

2.3 Multidimensional Scaling (MDS)

[36] is a classical dimensionality reduction technique that aims to preserve the pairwise Euclidean distances or dissimilarities between data points when projecting them into a lower-dimensional space. Given a distance matrix computed over the input space, MDS seeks a configuration of points in the target space such that their mutual distances approximate the original dissimilarities as closely

as possible. This makes MDS especially effective at uncovering the global geometric structure of data manifolds, and it has been widely used in applications such as psychometrics, bioinformatics, and visualization.

Classical MDS is typically implemented via eigendecomposition of the doubly centered distance matrix, which yields a set of coordinates corresponding to the principal axes of variation in the distance space. This spectral formulation ensures that MDS retains an interpretable, globally consistent embedding. However, it also introduces significant computational overhead: constructing and decomposing the full pairwise distance matrix incurs $\mathcal{O}(N^2)$ space and $\mathcal{O}(N^3)$ time complexity, making classical MDS unsuitable for large-scale datasets.

To address scalability and generalization, several out-of-sample extensions have been proposed. Regression-based methods [10, 45] allow new data points to be embedded in the learned low-dimensional space without recomputing the full distance matrix. These techniques typically fit a linear or non-linear model that maps high-dimensional inputs to their corresponding MDS coordinates, making it possible to apply MDS-style projections to streaming or test-time data.

Despite its theoretical elegance and historical significance, MDS suffers from practical limitations. Its reliance on exact distance preservation makes it highly sensitive to noise and outliers in the input space. Even small perturbations in distance values can significantly distort the resulting embeddings. Furthermore, for high-dimensional ANN or retrieval tasks, MDS does not explicitly optimize for neighborhood preservation, and the emphasis on global fidelity can misrepresent fine-grained local relationships—rendering it suboptimal for similarity search applications.

2.4 Random projections

[1, 48] are a class of lightweight and computationally efficient dimensionality reduction techniques based on the celebrated Johnson–Lindenstrauss (JL) lemma [14, 34]. The JL lemma asserts that any set of N points in high-dimensional Euclidean space can be embedded into a lower-dimensional space of dimension $\mathcal{O}(\log N/\epsilon^2)$ such that all pairwise distances are preserved up to a small distortion factor ϵ . Random projection methods operationalize this principle by multiplying the input data with a randomly generated matrix, typically populated with sub-Gaussian entries such as standard normal or sparsified ± 1 values [1]. The resulting transformation is linear, fast to compute, and requires no data-dependent training, making it highly scalable to large datasets.

Despite their simplicity and theoretical guarantees, random projections suffer from several practical limitations when applied to tasks such as approximate nearest neighbor (ANN) search. Their data-independence implies that the projection does not adapt to the structure or distribution of the input space, which can lead to suboptimal preservation of fine-grained geometric relationships—especially in datasets with strong clustering, anisotropic features, or manifold structure [7]. In particular, while inter-point distances may be roughly maintained, the relative neighborhood rankings—critical for retrieval performance—can be significantly distorted. Consequently, although random projections are valuable as a baseline or preprocessing step, they often underperform compared to more

sophisticated DR methods that incorporate task-aware or geometry-aware optimization.

3 MAXIMUM PAIRWISE ABSOLUTE DIFFERENCE

3.1 Overview

We propose a new dimensionality reduction method called *Maximum Pairwise Absolute Difference* (MPAD), designed to preserve local neighbor relationships in high-dimensional vector databases. Unlike traditional techniques such as PCA, which emphasize global variance, MPAD is tailored to maintain the local order structure that underlies k -Nearest Neighbor (k -NN) queries. The method defines a mapping $f : \mathbb{R}^n \rightarrow \mathbb{R}^m$ that seeks to maximize the smallest pairwise differences in scalar projections while discouraging redundancy among projection directions via a soft orthogonality penalty. This balance ensures that important local geometry is preserved without discarding meaningful directional overlap.

We will begin by formalizing domain and codomain notation (Table 1), along with evaluation metrics based on test sets and k -NN accuracy (Table 2). The core algorithm iteratively selects m projection directions by optimizing a signed objective function ϕ that balances informativeness and orthogonality. A key insight of MPAD is that preserving the smallest pairwise absolute differences among data projections helps maintain local structure in the reduced space. We analyze the method’s intuition, algorithmic formulation, and computational complexity in detail, and show that MPAD satisfies desirable mathematical properties such as boundedness, continuity, and monotonicity. These properties ensure the stability and interpretability of the approach and provide a rigorous foundation for its convergence guarantees.

To enable scalable application, we also provide a complexity analysis of both the sequential and parallel execution of MPAD, highlighting its suitability for large datasets under modern computational infrastructure. These features establish MPAD as a principled, flexible, and locally structure-preserving framework for dimensionality reduction in vector-based machine learning and database applications.

3.2 Notation

We consider a vector database of n -dimensional vectors, containing N data points. Our goal is to find a mapping:

$$f : \mathbb{R}^n \rightarrow \mathbb{R}^m$$

where $X \subseteq \mathbb{R}^n$, $f(X) = X' \subseteq \mathbb{R}^m$, and f is order-preserving.

We summarize the primary mathematical notations used in our dimensionality reduction framework in Table 1. The table defines both the domain and codomain of the transformation, the structure of the input and output vector sets, and their respective matrix representations. This formalism will be used consistently to describe the projection process, algorithmic objectives, and theoretical analysis in the sections that follow.

After defining the Order-Preserving Map f , we assess its performance using nearest neighbor preservation metrics. Table 2 introduces the notation used for evaluating the quality of the learned projection on unseen data. Specifically, the test set $Y \subset \mathbb{R}^n$ consists of d high-dimensional vectors that are not part of the training set.

Notation	Description
Domain \mathbb{R}^n	The n -dimensional Euclidean space (input space).
Codomain \mathbb{R}^m	The target space after dimensionality reduction, where $m < n$.
i-th input vector \mathbf{x}_i	The i -th vector in the domain, $\mathbf{x}_i \in \mathbb{R}^n$.
Input set $X = \{\mathbf{x}_i\}_{i=1}^N$	Collection of vectors to be reduced in dimensionality. Can also be treated as an $n \times N$ matrix (each column is \mathbf{x}_i^T).
i-th output vector \mathbf{x}'_i	The transformed vector in the codomain, where $f(\mathbf{x}_i) = \mathbf{x}'_i$.
Output set $X' = f(X) = \{\mathbf{x}'_i\}_{i=1}^N$	Collection of transformed vectors in the codomain. Can also be represented as an $m \times N$ matrix (each column is \mathbf{x}'_i^T).

Table 1: Notation and Definitions

These vectors are projected into the reduced space via the same mapping f learned from X , yielding the transformed test set $Y' \subset \mathbb{R}^m$. Each test vector \mathbf{y}_i is used to evaluate neighborhood preservation in the reduced space. We first compute the k -nearest neighbors of \mathbf{y}_i in the original space X , and then compare this neighborhood with the k -nearest neighbors of $f(\mathbf{y}_i)$ in the reduced set X' . This comparison provides the basis for our quantitative evaluation of local structure preservation under dimensionality reduction.

Notation	Description
Test set $Y = \{\mathbf{y}_i\}_{i=1}^d$	A set of test vectors in the domain \mathbb{R}^n of size d .
Mapped test set $Y' = f(Y)$	The transformed test set in the codomain.
i-th test vector \mathbf{y}_i	A test vector in Y , for which we find its k -NN in X , then map it to Y' and find its k -NN in X' .

Table 2: Test Set Notation

For a sufficiently large test set Y , the k -NN test accuracy is defined as:

$$\mathcal{A}_m(k) = \frac{\sum_{i=1}^d \# \text{ of } k \text{ nearest neighbors of } \mathbf{y}_i \text{ in the intersection of } X \text{ and } X'}{kd}.$$

- $\mathcal{A}_m(k) \in [0, 1]$.
- $\mathcal{A}_m(k) = 1$ if and only if f is order-preserving for k .
- Lower values indicate loss of original neighbors or introduction of spurious neighbors in X' .

We use $\mathcal{A}_m(k)$ to evaluate the performance of f .

3.3 Intuition

Dimensionality reduction techniques serve various objectives: some are designed to enhance classification performance, while some

others aim to capture the most significant variations in the data (e.g. PCA). Since any mapping from a high-dimensional space to a lower-dimensional one must inevitably discard some information in general, the challenge is to determine which aspects of the data can be approximated and which must be preserved.

Motivated by the need to retain critical structural information, we focus on preserving the local order of data points—specifically, the k -Nearest Neighbor relationships under the L_p norm.

Our approach begins with a fundamental question: if we are to select a single axis (or dimension) in \mathbb{R}^n on which to project the input set X , which axis should we choose? A natural answer is to select the axis along which the data exhibits the greatest variance, as in Principal Component Analysis (PCA), thereby maximizing the separation between data points. However, three key limitations of PCA in preserving local order become evident:

Information Trade-offs: Emphasizing variance may obscure subtle but important details.

Local versus Global Structure: In many applications, maintaining the integrity of local neighborhoods (i.e., preserving the nearest k neighbors) is more crucial than capturing global variance.

Emphasis on Pairwise Differences: The L_p distance between two vectors,

$$\|\mathbf{x}_i - \mathbf{x}_j\|_p = \left(\sum_{k=1}^n |x_{ik} - x_{jk}|^p \right)^{\frac{1}{p}},$$

suggests that examining the dimension-wise absolute differences can reveal a more fundamental structure than variance alone.

In light of these insights, our method selects the dimension that maximizes the average of the smallest $b\%$ of the pairwise absolute differences. Denote by \mathbf{e}_k the standard basis vectors in \mathbb{R}^n . The projection of a point $\mathbf{x}_i \in X$ onto the axis defined by \mathbf{e}_k is given by

$$f_{\mathbf{e}_k}(\mathbf{x}_i) = (\mathbf{e}_k \cdot \mathbf{x}_i) \mathbf{e}_k.$$

For each pair $1 \leq i < j \leq N$, we define the projected difference as

$$d_{ij} = |\mathbf{e}_k \cdot (\mathbf{x}_i - \mathbf{x}_j)|.$$

Let D_b be the set of the smallest $b\%$ of these differences:

$$D_b = \{d_{ij} \mid d_{ij} \text{ is among the smallest } b\% \text{ of all pairwise differences}\}.$$

Our objective is to choose the basis vector \mathbf{e}_k that maximizes

$$\max_{\mathbf{e}_k} \frac{1}{|D_b|} \sum_{d_{ij} \in D_b} d_{ij}.$$

This criterion is designed to preserve the local order structure that is essential for accurate k -Nearest Neighbor results in the reduced space.

High-dimensional datasets often exhibit characteristics that both complicate dimensionality reduction and highlight the advantages of our MPAD method:

Concentration of Measure: In high dimensions, pairwise distances tend to become nearly uniform, complicating the differentiation between close and distant points.

Redundancy: Typically, only a few dimensions contain most of the discriminative information, while the remainder may contribute noise or redundancy.

Dominance of Local Structure: The intrinsic organization of the data is frequently governed by local relationships rather than by

global variance, making it imperative to preserve the finer details of the nearest neighbor topology.

3.4 Algorithm

We first propose our method here, with more rigorous mathematical analysis in the next section.

Given n as the dimension of the domain, m as the dimension of the codomain, and X as the set of vectors whose dimensionality we want to reduce, we want to find m vectors in \mathbb{R}^n and project X onto each of the m selected vectors. Then X' lies in the space generated by these m vectors, i.e. \mathbb{R}^m .

- (1) Generate the first basis vector of \mathbb{R}^m . Calculate $b\%$ MPAD(\mathbf{w}_1) = $\mu_b(\mathbf{w}_1)$. Let \mathbf{w}_1 be a random unit vector in \mathbb{R}^n , and let X' be the projection of X onto \mathbf{w}_1 (i.e.,

$$f_{\mathbf{w}_1}(\mathbf{x}_i) = \text{proj}_{\mathbf{w}_1}(\mathbf{x}_i) = \langle \mathbf{x}_i, \mathbf{w}_1 \rangle \mathbf{w}_1,$$

which projects each $\mathbf{x}_i \in X$ onto \mathbf{w}_1). For all $1 \leq i < j \leq N$, define

$$d_{1,ij} = \left\| f_{\mathbf{w}_1}(\mathbf{x}_i) - f_{\mathbf{w}_1}(\mathbf{x}_j) \right\|.$$

Let $b \in (0, 100]$ and define the set

$$D_{1,b} = \{d_{1,ij} \mid \text{Smallest } b\% \text{ of } d_{1,ij}\}.$$

We then define

$$\mu_b(\mathbf{w}_1) = \frac{1}{|D_{1,b}|} \sum_{d_{1,ij} \in D_{1,b}} d_{1,ij}.$$

We want to select

$$\arg \max_{\mathbf{w}_1} \mu_b(\mathbf{w}_1) = \arg \max_{\mathbf{w}_1} \frac{1}{|D_{1,b}|} \sum_{d_{1,ij} \in D_{1,b}} d_{1,ij}$$

as the first basis vector of \mathbb{R}^m .

- (2) For the second basis vector \mathbf{w}_2 , we assign an orthogonality penalty to its direction, as we wish to separate its direction from \mathbf{w}_1 to preserve as much information as possible. Notice that although we assign an orthogonality penalty, we do not force \mathbf{w}_2 to be orthogonal to \mathbf{w}_1 like in PCA. This is because we believe that in many real-life scenarios some directions indeed convey more information than others, and there is no reason to force them to be orthogonal. We assign the penalty for \mathbf{w}_2 as

$$P_{\text{orth},2} = \alpha (\mathbf{w}_1 \cdot \mathbf{w}_2)^2.$$

The parameter α is a penalizing factor in $(0, \infty)$ used to adjust the strength of the penalty.

The process of calculating $\mu_b(\mathbf{w}_2)$ is similar to Step 1. Then we want to find

$$\begin{aligned} & \arg \max_{\mathbf{w}_2} (\mu_b(\mathbf{w}_2) - P_{\text{orth},2}) \\ &= \arg \max_{\mathbf{w}_2} \left(\frac{1}{|D_{2,b}|} \sum_{d_{2,ij} \in D_{2,b}} d_{2,ij} - \alpha (\mathbf{w}_1 \cdot \mathbf{w}_2)^2 \right). \end{aligned}$$

- (3) For the k -th basis vector \mathbf{w}_k , we assign the penalty

$$P_{\text{orth},k} = \alpha \sum_{i=1}^{k-1} (\mathbf{w}_i \cdot \mathbf{w}_k)^2.$$

And we want to find

$$\begin{aligned} & \arg \max_{\mathbf{w}_k} (\mu_b(\mathbf{w}_k) - P_{\text{orth},k}) \\ &= \arg \max_{\mathbf{w}_k} \left(\frac{1}{|D_{k,b}|} \sum_{d_{k,ij} \in D_{k,b}} d_{k,ij} - \alpha \sum_{i=1}^{k-1} (\mathbf{w}_i \cdot \mathbf{w}_k)^2 \right). \end{aligned}$$

- (4) Repeat until all m basis vectors have been selected. They will generate the codomain \mathbb{R}^m . Then we define f to be the projection map:

$$f: \mathbb{R}^n \rightarrow \mathbb{R}^m, \quad f(\mathbf{x}) = (\langle \mathbf{x}, \mathbf{w}_1 \rangle, \langle \mathbf{x}, \mathbf{w}_2 \rangle, \dots, \langle \mathbf{x}, \mathbf{w}_m \rangle), \quad \forall \mathbf{x} \in \mathbb{R}^n.$$

In matrix terms, if we let $M_{m \times n}$ be an $m \times n$ matrix whose i -th row is \mathbf{w}_i^T , then $f(\mathbf{x}) = M\mathbf{x}$, and $f(X) = MX$.

3.5 Analysis

Time Complexity. We now analyze the computational complexity of the proposed algorithm and examine opportunities for parallel computation. Let us revisit each primary computational step in the method and quantify its complexity. Assume:

- N : number of data points (vectors).
- n : dimensionality of the domain (Input set).
- m : dimensionality of the codomain (Output set).
- T : number of iterations required for convergence in optimization.
- b : fraction (percentage) of smallest pairwise distances considered.

We examine each step individually:

Generation of Pairwise Projections and Distances: For each candidate vector \mathbf{w}_k , the projection of all N vectors onto \mathbf{w}_k involves a dot product for each vector, yielding complexity $O(N \cdot n)$. After projection, computing all pairwise distances has complexity $O(N^2)$. Selecting the smallest $b\%$ of these distances involves sorting, which takes $O(N^2 \log N^2) \rightarrow O(N^2 \log N)$. Since we perform this step for each of the m basis vectors, the complexity is:

$$O(m \cdot (N \cdot n + N^2 \log N)).$$

Orthogonality Penalty Calculation: For the k -th vector, calculating the orthogonality penalty with respect to previously chosen $(k-1)$ vectors involves $(k-1)$ dot products, each with complexity $O(n)$. Across all m vectors, this yields complexity $O(m^2 \cdot n)$. Typically, since $m \ll N$, this complexity is negligible compared to the previous step.

Optimization Iterations: Optimization to determine each \mathbf{w}_k is iterative. Suppose each optimization step involves a constant number of candidate evaluations. Denoting the average iterations per vector as T , the complexity multiplies by T :

$$O(m \cdot T \cdot (N \cdot n + N^2 \log N)).$$

Thus, the overall complexity of our algorithm is dominated by $O(N^2 \log N)$, given that we would usually expect that $N \gg n$, $N \gg m$, and $N \gg T$, which may become computationally intensive for large datasets.

Algorithm 1 MPAD

Input: Data set $X = \{\mathbf{x}_i\}_{i=1}^N \subset \mathbb{R}^n$, target dimension m , orthogonality penalty factor α , fraction $b \in (0, 100]$, and number of optimization iterations limit T

Output: Projection matrix $M \in \mathbb{R}^{m \times n}$ and mapping $f(\mathbf{x}) = M\mathbf{x}$

- 1: Initialize $M \leftarrow []$
- 2: **for** $k = 1$ **to** m **do**
- 3: Initialize candidate basis vector \mathbf{w}_k as a random unit vector in \mathbb{R}^n
- 4: **for** $t = 1$ **to** T **do**
- 5: **Projection:** For each $\mathbf{x}_i \in X$, compute scalar projection $p_i = \langle \mathbf{x}_i, \mathbf{w}_k \rangle$
- 6: **Pairwise Distances:** For all $1 \leq i < j \leq N$, compute
$$d_{ij} = |p_i - p_j|$$
- 7: Sort all d_{ij} and select the smallest $b\%$ to form the set $D_{k,b}$
- 8: Compute utility:
$$\mu_b(\mathbf{w}_k) = \frac{1}{|D_{k,b}|} \sum_{d_{ij} \in D_{k,b}} d_{ij}$$
- 9: **if** $k > 1$ **then**
- 10: Compute orthogonality penalty:
$$P_{\text{orth},k} = \alpha \sum_{i=1}^{k-1} (\mathbf{w}_i \cdot \mathbf{w}_k)^2$$
- 11: **else**
- 12: Set $P_{\text{orth},k} \leftarrow 0$
- 13: **end if**
- 14: **Objective:** Define
$$\phi(\mathbf{w}_k) = \mu_b(\mathbf{w}_k) - P_{\text{orth},k}$$
- 15: Update \mathbf{w}_k using an optimization method (e.g., gradient ascent) to maximize $\phi(\mathbf{w}_k)$
- 16: **end for**
- 17: Append the optimized \mathbf{w}_k as the k -th row of M
- 18: **end for**
- 19: **return** M , with mapping $f(\mathbf{x}) = M\mathbf{x}$

Space Complexity. The space complexity of the algorithm is primarily determined by the storage required for computing and managing the pairwise distances among the projected vectors. We analyze the key components as follows:

Projection Storage: For each candidate basis vector \mathbf{w}_k , projecting the input set X of N vectors yields an array of N scalar values. This requires $O(N)$ space.

Pairwise Distances: The most memory-intensive step involves calculating the pairwise distances among the N projected values. Since there are roughly $\binom{N}{2} = O(N^2)$ distinct pairs, storing these distances requires $O(N^2)$ space.

Basis Vectors: The algorithm stores m basis vectors, each of dimension n . This adds an extra $O(m \cdot n)$ space. Typically, since $N \gg m$ and n is moderate, this term is negligible compared to $O(N^2)$.

Thus, in the worst-case scenario, the overall space complexity of the algorithm is dominated by the pairwise distance storage $O(N^2)$. It is worth noting that if one employs streaming methods or in-place selection techniques for determining the smallest $b\%$ distances, the practical memory footprint can be reduced. However, in the worst-case analysis, the space complexity remains $O(N^2)$.

Ideal Parallel Computation with P Processors. Assume we have P processors available. Under the assumption of perfect load balancing, the heavy computations can be parallelized as follows:

Parallel Projection: The projection of N vectors onto a candidate basis vector, which requires $O(N \cdot n)$ operations sequentially, can be distributed over P processors. This reduces the time to $O\left(\frac{N \cdot n}{P}\right)$.

Parallel Distance Calculation: Computing all N^2 pairwise distances, originally costing $O(N^2)$ operations, can be carried out in $O\left(\frac{N^2}{P}\right)$ time when distributed evenly across P processors.

Parallel Sorting: The time needed for sorting the N^2 pairwise distances using an optimal parallel sorting algorithm is of

$$O\left(\frac{N^2}{P} \log(N^2)\right) \rightarrow O\left(\frac{N^2}{P} \log N\right).$$

Thus, for each optimization iteration per candidate basis vector, the dominant cost is due to sorting, requiring

$$O\left(\frac{N^2}{P} \log N\right).$$

If T iterations are needed per basis vector, the time per candidate becomes

$$O\left(T \cdot \frac{N^2}{P} \log N\right).$$

Since the selection of basis vectors is inherently sequential (due to dependencies introduced by the orthogonality penalty), the overall ideal parallel time complexity of the algorithm is:

$$O\left(m \cdot T \cdot \frac{N^2}{P} \log N\right).$$

Again, we expect that $N \gg m$ and $N \gg T$, so the complexity reduce to

$$O\left(\frac{N^2}{P} \log N\right).$$

Summary of Time Complexity. Table 3 summarizes the time complexities of our proposed MPAD method under sequential and ideal parallel conditions, alongside those of several standard dimensionality reduction methods.

The linear reduction in computational time under ideal parallelization underscores the potential of leveraging modern parallel computing architectures for large-scale applications.

3.6 Theoretical Properties

We will show that MPAD satisfies some desired mathematical properties and why those properties are meaningful. Notice that MPAD is built upon the objective function, which is a signed measure, as

$$\phi(\{\mathbf{w}_k\}_{k=1}^m) = \sum_{k=1}^m \left[\mu_b(\mathbf{w}_k) - \alpha \sum_{j=1}^{k-1} (\mathbf{w}_j \cdot \mathbf{w}_k)^2 \right],$$

Method	Time Complexity
MPAD (Sequential)	$O(N^2 \log N)$
MPAD (Ideal Parallel, P processors)	$O\left(\frac{N^2}{P} \log N\right)$
PCA	$O(N \cdot n^2)$
Kernel PCA	$O(N^3)$
MDS	$O(N^3)$
Isomap	$O(N^3)$
UMAP	$O(N \log N)$

Table 3: Comparison of time complexities for MPAD and some mainstream DR methods.

where the utility function is defined as

$$\mu_b(\mathbf{w}_k) = \frac{1}{|D_{k,b}|} \sum_{d_{k,i,j} \in D_{k,b}} d_{k,i,j}, \quad d_{k,i,j} = \left| \mathbf{w}_k \cdot (\mathbf{x}_i - \mathbf{x}_j) \right|.$$

Objective Function ϕ being a Signed Measure. Defining ϕ as a *signed measure* is more than a mathematical formality—it provides a structured way to assess and decompose the quality of our basis vectors. First, the measure ϕ naturally splits into positive contributions, via $\mu_b(\mathbf{w}_k)$ (which quantifies the preservation of local neighborhood order), and negative contributions, via the orthogonality penalty. This decomposition allows us to **analyze how each basis vector improves or degrades** the overall preservation of the k -NN structure. Second, through the property of countable additivity (detailed below), we can **assess the effect of subsets of basis vectors independently**. This modularity is valuable when designing algorithms, as it **enables parallel optimization and local performance analysis** that aggregates to a global measure. Besides, a measure-theoretic foundation ensures that every part of our objective is derived from well-defined mathematical principles. In this way, we **avoid arbitrary choices** in the design of the method, thereby ensuring **consistency and reproducibility**.

Other Mathematical Properties: Boundedness, Compactness, Continuity, and Monotonicity. These mathematical properties are not merely theoretical conveniences—they are essential to ensuring the practical reliability of our proposed dimensionality reduction algorithm. *Boundedness* guarantees that the optimization objective remains **well-defined and numerically stable across iterations**. *Compactness* ensures the **existence of optima**, preventing divergence or undefined behavior. *Continuity* **allows gradient-based or continuous optimization strategies** to be applicable, as small changes in the parameters yield predictable changes in the objective. Finally, *monotonicity* provides a formal assurance that the algorithm will improve or maintain performance at every step, thereby **ensuring convergence**. Together, these properties lay a robust theoretical foundation for the correctness and stability of the approach. Below we elaborate on these key properties and provide supporting equations and reasoning.

Proofs of the above properties.

PROOF OF BOUNDEDNESS. Each basis vector \mathbf{w}_k is constrained to lie on the unit sphere in \mathbb{R}^n , i.e., $\|\mathbf{w}_k\| = 1$. For any two vectors

$\mathbf{x}_i, \mathbf{x}_j \in X$, by the Cauchy–Schwarz inequality,

$$\left| \mathbf{w}_k \cdot (\mathbf{x}_i - \mathbf{x}_j) \right| \leq \|\mathbf{w}_k\| \cdot \|\mathbf{x}_i - \mathbf{x}_j\| = \|\mathbf{x}_i - \mathbf{x}_j\|.$$

Let $D_{max} = \max_{i,j} \|\mathbf{x}_i - \mathbf{x}_j\|$.

Then, for every \mathbf{w}_k , we have $\mu_b(\mathbf{w}_k) \leq D_{max}$. Similarly, since $(\mathbf{w}_j \cdot \mathbf{w}_k)^2 \leq 1$, the penalty term satisfies

$$P_{\text{orth},k} = \alpha \sum_{j=1}^{k-1} (\mathbf{w}_j \cdot \mathbf{w}_k)^2 \leq \alpha(k-1).$$

Thus, for m basis vectors,

$$\phi(\{\mathbf{w}_k\}_{k=1}^m) \leq mD_{max} - \alpha \sum_{k=1}^m (k-1) = mD_{max} - \alpha \frac{m(m-1)}{2}.$$

This upper bound (and a corresponding lower bound) ensures that ϕ is bounded. \square

PROOF OF COMPACTNESS. The set of candidate basis vectors is the unit sphere S^{n-1} , which is compact in \mathbb{R}^n . Since continuous functions on compact sets are bounded and attain their extrema, if the operations defining ϕ were entirely continuous, then ϕ would be guaranteed to have a maximum and minimum. Although the sorting operation in the definition of μ_b can introduce discontinuities, these occur only at isolated points (a measure-zero set), thus preserving the overall compact behavior of the domain. \square

PROOF OF CONTINUITY. Consider the projection function $f_{\mathbf{w}}(\mathbf{x}) = \langle \mathbf{x}, \mathbf{w} \rangle$.

This function is continuous in \mathbf{w} because the dot product is linear. The absolute value function and finite sums are also continuous. Hence, for almost every \mathbf{w}_k ,

$$\mu_b(\mathbf{w}_k) = \frac{1}{|D_{k,b}|} \sum_{d_{k,i,j} \in D_{k,b}} \left| \langle \mathbf{x}_i - \mathbf{x}_j, \mathbf{w}_k \rangle \right|$$

is continuous except at those critical points where the order of pairwise distances changes. The penalty term,

$$P_{\text{orth},k} = \alpha \sum_{j=1}^{k-1} (\mathbf{w}_j \cdot \mathbf{w}_k)^2,$$

is a polynomial function in the entries of \mathbf{w}_k and is therefore continuous. Overall, the function ϕ is (almost everywhere) continuous on the compact domain. \square

PROOF OF MONOTONICITY. In our algorithm, each update step for \mathbf{w}_k is performed with the goal of increasing the objective

$$J(\mathbf{w}_k) = \mu_b(\mathbf{w}_k) - P_{\text{orth},k}.$$

Thus, at each iteration t , we have $\phi^{(t+1)} \geq \phi^{(t)}$.

Since ϕ is bounded above (as shown under Boundedness), the monotonic sequence $\{\phi^{(t)}\}$ must converge. This monotonicity is crucial to guarantee algorithmic stability and convergence in practice. \square

We then show that ϕ behaves like a signed measure.

PROOF OF SIGNED MEASURE PROPERTIES. It is sufficient to prove that:

Null Empty Set. For an empty collection of basis vectors, the convention for empty sums gives

$$\phi(\emptyset) = \sum_{k \in \emptyset} \left[\mu_b(\mathbf{w}_k) - \alpha \sum_{j=1}^{k-1} (\mathbf{w}_j \cdot \mathbf{w}_k)^2 \right] = 0.$$

Countable Additivity. Let $B = \{\mathbf{w}_i\}_{i \in I}$ be a countable set of basis vectors. Suppose we partition B into disjoint subsets $\{B_k\}_{k \in \mathbb{N}}$ such that

$$B = \bigcup_{k \in \mathbb{N}} B_k, \quad B_k \cap B_\ell = \emptyset \text{ for } k \neq \ell.$$

For each subset B_k , define

$$\phi(B_k) = \sum_{\mathbf{w} \in B_k} \mu_b(\mathbf{w}) - \alpha \sum_{\substack{\mathbf{v}, \mathbf{w} \in B_k \\ \mathbf{v} \text{ precedes } \mathbf{w}}} (\mathbf{v} \cdot \mathbf{w})^2.$$

By choosing an ordering where vectors in each B_k appear consecutively, we have

$$\phi\left(\bigcup_{k \in \mathbb{N}} B_k\right) = \sum_{k \in \mathbb{N}} \phi(B_k).$$

This confirms the countable additivity property of ϕ . \square

4 EVALUATION

In this section, we assess the performance of our proposed MPAD method against several established dimensionality reduction techniques on datasets in various areas.

4.1 Datasets and Setup

Dataset. We evaluate our method on four diverse datasets spanning different domains: Fasttext [8, 25, 26] (text), Isolet [12] (voice), Arcene [18] (human health/mass-spectrometry), and PBMC3k [40] (biology/genomics). The Fasttext dataset consists of pre-trained word vectors; in our experiments, we use the wiki-news-300d-1M model, which comprises one million vectors trained on Wikipedia 2017, the UMBC webbase corpus, and the statmt.org news dataset (16B tokens). The Isolet dataset includes recordings from 150 subjects, each pronouncing the name of every letter of the alphabet twice. We use the designated training set (isolet1+2+3+4), making it well-suited for noisy, perceptual tasks and for testing the scaling abilities of various algorithms. The Arcene dataset, created for the NIPS 2003 feature selection challenge, comprises mass-spectrometry data used to distinguish between cancerous and healthy patients; we employ its training, validation, and test splits. The PBMC3k dataset contains single-cell RNA sequencing data from approximately 3,000 peripheral blood mononuclear cells (PBMCs) from a healthy human donor. It is commonly used to benchmark and investigate immune cell types and gene expression patterns in scRNA-seq analyses. For this dataset, we utilize the non-empty points from the pbmc3k_processed data provided by Scanpy. Table 4 summarizes the key characteristics of these four datasets.

Parameters. Our experiments consider four parameters. Two global parameters affect all baseline methods: the Target Ratio (defined as the ratio of the target dimension to the input dimension) and the neighborhood size k . Throughout our experiments, we use

Target Ratios of [0.05, 0.1, 0.2, 0.4, 0.6] and neighborhood sizes of [1, 3, 6, 10, 15]. Additionally, the MPAD method introduces two specific parameters: α , which controls the penalty on non-orthogonality, and b , which governs the preservation of the local data manifold. We sweep α over [1, 6, 12, 18, 25, 35, 50, 10000] and b over [60, 70, 80, 90, 100]. It is worth noting that assigning $\alpha = 10000$ essentially enforce the select projection vectors to be orthogonal. Consequently, for each dataset, we conduct exactly 1000 accuracy tests across different parameter combinations.

Metrics. The primary performance metric is the k -NN test accuracy, denoted as $\mathcal{A}_m(k)$, which quantifies how well local neighborhood relationships are preserved in the reduced space for an external test set. We use a different seed to randomly select 600 points (297 points for Arcene, limited by the dataset size) from each dataset as the test set Y , and calculate $\mathcal{A}_m(k)$ as described in the section 3.2. Additionally, we record the frequency with which each method ranks as the best or second-best performer, serving as an auxiliary measure of the robustness of MPAD and the baseline methods.

Baseline. We compare MPAD against several baseline dimensionality reduction methods: UMAP [35], Isomap [44], Kernel PCA [42], and Multidimensional Scaling (MDS) with a linear regression-based out-of-sample extension [10, 45]. Although Kernel PCA is more computationally expensive than PCA, its ability to capture non-linear structures makes it a more accurate and robust baseline—hence its inclusion instead of standard PCA. Furthermore, because MDS does not inherently support out-of-sample dimensionality reduction, we first apply MDS to the input set and then learn the projection mapping using a linear regression model.

Environment. All experiments are implemented in Python and executed on CloudLab using machines running Ubuntu 22.04.2 LTS (GNU/Linux 5.15.0-131-generic x86_64). Each node is equipped with two AMD EPYC 7543 32-core processors running at 2.80GHz, 256GB of ECC memory (16×16GB 3200MHz DDR4), a 480GB SATA SSD, and a 1.6TB NVMe SSD (PCIe v4.0). MPAD computations and nearest neighbor searches are accelerated through parallel processing across CPU cores.

4.2 Evaluation on Overall Effectiveness

We want to first evaluate the overall performance of the MPAD method. We want to compare the average performance of MPAD (using a single fixed combination of (α, b) per dataset) against the **baseline methods** for various target ratios (i.e., different reduced dimensionalities) and different neighborhood sizes k . Specifically, we choose a **fixed** pair of parameter values (α, b) for MPAD for each dataset. Then we compute the accuracy $\mathcal{A}_m(k)$ for each target ratio and k combination and take the average of different $\mathcal{A}_m(k)$ to assess the average performance $\bar{\mathcal{A}}_m(k)$ of different DR methods.

To assess the overall retrieval-oriented effectiveness of MPAD, we evaluate its average performance across varying global parameters—specifically, target dimensionality ratios and neighborhood sizes k . For each dataset, we select a single (α, b) configuration for MPAD and compare its performance against four widely used dimensionality reduction baselines: UMAP, Isomap, Kernel PCA (KPCA), and MDS with linear-regression based out-of-sample projection.

Table 4: Dataset Characteristics

Dataset	Domain	Total Dimension	Total Size	Sample Dimension	Sample Size	Sampling
Fasttext	Text	300	1,000,000	300	600	Random
Isolet	Voice	617	7,797	200	600	Random
Arcene	Health/Mass-spectrometry	10000	900	200	600	Random
PBMC3k_Processed	Biology/Genomics	1838	2638	200	600	Random

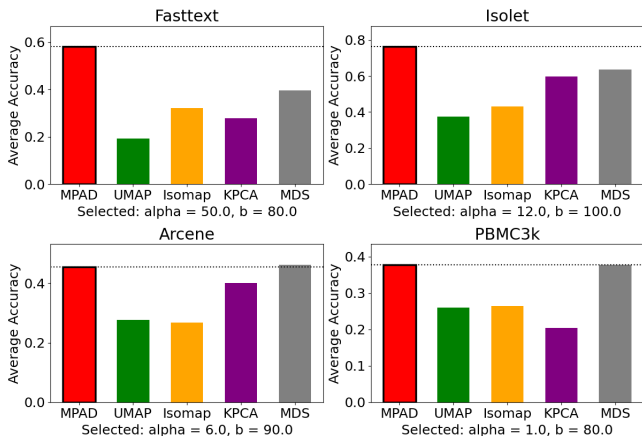


Figure 1: Average k -NN accuracy $\overline{\mathcal{A}_m(k)}$ across all target ratios and neighborhood sizes for each dataset. MPAD consistently achieves the highest or second-highest performance compared to baseline methods.

Figure 1 presents the **average k -NN accuracy $\overline{\mathcal{A}_m(k)}$** across combinations of k and target dimension ratios. The results clearly show that MPAD consistently yields the highest or second-highest accuracy on all four datasets. On Fasttext and Isolet, MPAD significantly outperforms all baselines, reflecting its strong alignment with neighborhood-preserving objectives in both text and auditory domains. The selected parameter combinations (e.g., $\alpha = 50.0, b = 80.0$ for Fasttext) ensure robustness over a wide range of retrieval settings without requiring per-instance tuning.

In the Arcene dataset—representing high-dimensional biomedical data—MPAD maintains a clear lead over manifold-based methods like UMAP and Isomap, while performing on par with MDS. Notably, MDS also shows competitive results across several datasets, particularly Arcene and PBMC3k. This suggests that in settings lacking strong nonlinear manifold structure, simpler global geometry-preserving approaches like MDS may offer surprisingly strong performance, likely due to their fewer assumptions and smooth linear behavior.

The PBMC3k dataset poses a more challenging scenario due to its sparse and noisy nature from single-cell RNA-seq data. Even in this setting, MPAD remains competitive, closely matching MDS in overall accuracy. KPCA, while occasionally strong (e.g., in Isolet), suffers in noisier or less structured datasets due to its sensitivity to kernel choice and parameterization.

Overall, MPAD achieves strong average neighborhood-preserving accuracy in all domains tested. Its consistent performance under

a fixed parameter configuration highlights its practicality in real-world retrieval pipelines, where per-query or per-dataset tuning is often infeasible. These findings validate our hypothesis that a margin-based, order-preserving objective tailored for approximate nearest-neighbor retrieval leads to better global OPDR performance than traditional variance- or topology-driven approaches.

4.3 Evaluation on Robustness

While the previous subsection focused on MPAD’s average performance using a single parameter configuration, we now investigate how *robust* MPAD is across its entire parameter space. Recall that MPAD introduces two additional hyperparameters: α , which controls the penalty for non-orthogonality, and b , which determines the fraction of smallest pairwise distances used in the objective. We sweep α over 8 values and b over 5 values, resulting in 40 MPAD configurations. Combined with 25 global parameter combinations (five target ratios and five k -NN sizes), we obtain a total of 1000 experimental settings per dataset. For each setting, we fix an MPAD configuration (α, b) , choose a target dimension ratio and neighborhood size k , and compute the k -NN accuracy $\mathcal{A}_m(k)$. We compare the result against the four baseline methods (UMAP, Isomap, KPCA, and MDS) and record which method achieves the best and second-best accuracy. Repeating this process across all parameter combinations allows us to count how often each method ranks first or second.

Figure 2 shows the results. Each subplot corresponds to one dataset, and each stacked bar reports the number of times a method achieves the highest or second-highest accuracy. MPAD dominates across most datasets, achieving the most first-place finishes in nearly every scenario. It also consistently appears as the second-best method in the remaining cases. In contrast, the other methods—while occasionally competitive—lack this level of consistency across the full parameter space.

These findings demonstrate that MPAD is not only effective but also highly robust. Its performance does not hinge on finely tuned parameter choices, which is critical in real-world deployments where exhaustive hyperparameter searches may be impractical. Even under diverse conditions, MPAD consistently preserves nearest-neighbor structure better than existing baseline dimensionality reduction techniques.

4.4 Ablation Study

To further understand the behavior of MPAD, we conduct an ablation study to examine how different parameter choices affect its performance. Specifically, we isolate each parameter of interest and systematically vary it while holding all other parameters fixed, including the target dimension. We then record the changes in k -NN

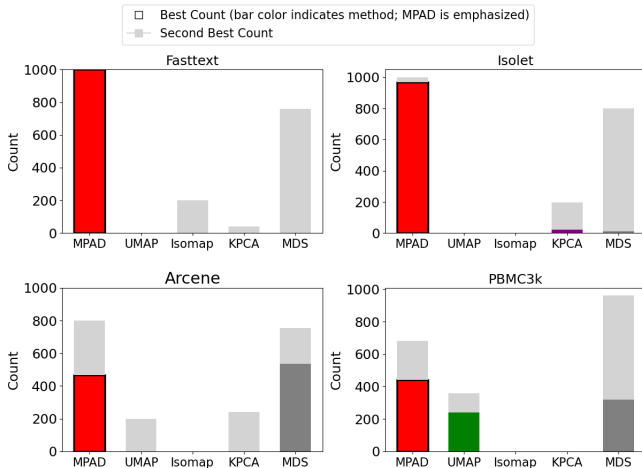


Figure 2: Robustness of MPAD measured by the number of times each method ranks first or second in accuracy across all MPAD parameter combinations. MPAD dominates across all datasets, indicating strong stability and broad effectiveness.

accuracy $\mathcal{A}_m(k)$ and compare MPAD’s behavior against that of baseline methods.

Figure 3 presents representative ablation results for each of the four datasets. Each row corresponds to a dataset, and each column isolates a different parameter. From left to right, the plots show the effect of varying neighborhood size k , target dimension ratio, the parameter b (which controls the fraction of pairwise distances used in the MPAD objective), and the orthogonality penalty α . For each plot, the baseline parameter configuration is noted in the title. Across all datasets, MPAD consistently outperforms baseline methods across most parameter settings.

In the first column (varying k), MPAD demonstrates strong relative accuracy overall. It maintains high accuracy across all k values, in contrast to methods like Isomap, whose performance fluctuates significantly with different k . This stability suggests that one can reasonably estimate performance at other k values in ANN search tasks by evaluating just a single or only a few k values. Notably, MPAD’s relative advantage is even more pronounced at small k values—a particularly important feature, as many real-world ANN search tasks prioritize retrieving only the top-1 or top-3 neighbors. Unlike some baselines that become competitive only at larger k , MPAD preserves its performance edge even in these more demanding settings.

In the second column (target ratio), MPAD demonstrates a clear upward trend: its k -NN accuracy improves steadily as the target dimension increases. This monotonicity is desirable in practice, as it provides users with a stable and interpretable trade-off: increasing the target dimension will consistently lead to better recall. In contrast, UMAP sometimes experience *decreasing* accuracy as the target ratio increases. This counterintuitive behavior is likely due to overfitting or noise amplification in the manifold assumptions used by those methods.

In the third and fourth columns, we vary MPAD’s internal parameters b and α , respectively. While accuracy does fluctuate, MPAD

remains consistently strong across wide ranges of these values. This suggests that MPAD is not overly sensitive to parameter tuning—users can obtain good performance without exhaustive search. In particular, accuracy tends to plateau for α beyond a moderate threshold, indicating stability in the orthogonality penalty.

Overall, this ablation study shows that MPAD is not only accurate but also interpretable and dependable. Its behavior aligns with intuitive expectations: higher target dimensions lead to better accuracy; small k -NN tasks remain tractable; and parameter robustness ensures ease of deployment. These properties distinguish MPAD from more brittle alternatives whose performance may vary significantly under minor parameter changes.

5 ADDITIONAL RELATED WORK

5.1 Manifold Learning and Visualization-Driven Dimensionality Reduction

Several methods have been designed to uncover low-dimensional manifolds embedded in high-dimensional space. Compared to classical linear methods, they are often more computationally expensive but also more powerful in preserving topological structures and visual coherence.

Isomap [6, 44] extends MDS by preserving geodesic distances rather than straight-line Euclidean distances. It constructs a neighborhood graph and estimates pairwise geodesics using shortest path algorithms. This allows the embedding to reflect the true geometry of a non-linear manifold. However, its dependency on k -NN graph construction and shortest-path computation renders it impractical for large-scale datasets [4].

Locally Linear Embedding (LLE)[39] is based on the premise that each data point and its neighbors lie on a locally linear patch of the manifold. It reconstructs each point using a linear combination of its neighbors, and then finds a low-dimensional embedding that preserves these reconstruction weights. Though theoretically appealing, LLE assumes noise-free data and can exhibit instability in the presence of sparse or high-dimensional samples[41].

t-SNE (t-distributed Stochastic Neighbor Embedding)[46] maps high-dimensional data to a low-dimensional space by minimizing the Kullback–Leibler divergence between probability distributions that reflect neighborhood similarities. **UMAP (Uniform Manifold Approximation and Projection)**[35] is a more recent technique that uses a fuzzy topological structure to achieve similar goals with better runtime scalability. Both methods excel at visualization and cluster separation but significantly distort global distances and are unsuitable for tasks requiring metric preservation or nearest-neighbor retrieval.

5.2 High-Dimensional Indexing and ANN Search

ANN search complements DR by enabling efficient retrieval in high-dimensional settings. However, most indexing methods assume fixed embeddings and do not alter dimensionality to preserve neighbor structure.

Locality-Sensitive Hashing (LSH) [13, 16, 22] offers a probabilistic solution to approximate nearest neighbor (ANN) search by designing hash functions that map similar items to the same

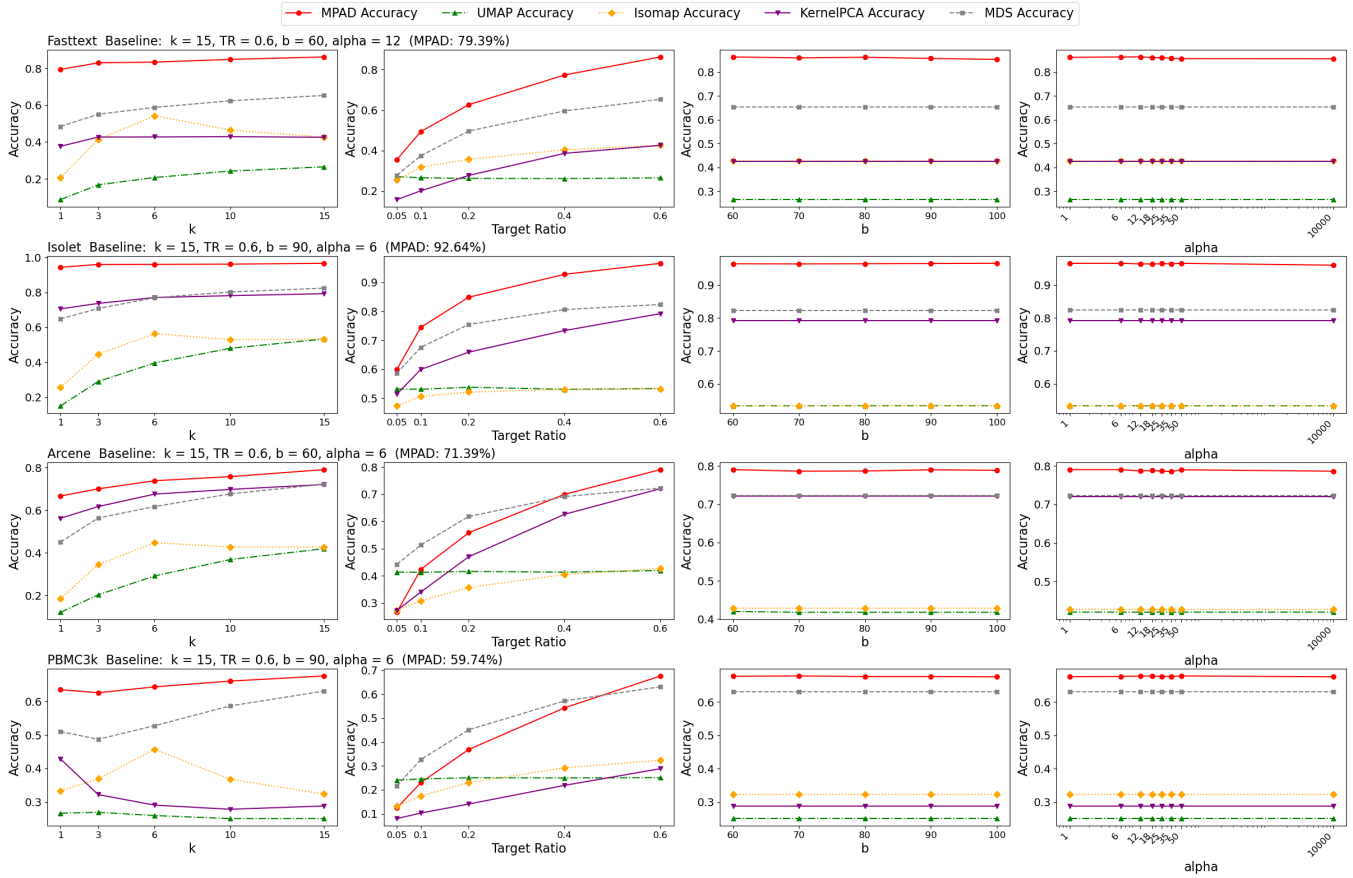


Figure 3: Ablation Study. Each subplot visualizes the effect of varying one parameter (e.g., k , target ratio, b , or α), with all others fixed. MPAD consistently maintains strong performance across a broad parameter range. The baseline parameter combinations are listed for each dataset.

bucket with high probability. It provides theoretical guarantees for sublinear query time and has been widely adopted in large-scale vector retrieval systems. LSH is often combined with random projections to reduce dimensionality prior to hashing, further improving efficiency. Despite its practical success, LSH has notable limitations: its hashing mechanism introduces quantization effects that can distort fine-grained geometric relationships, making it difficult to preserve nuanced similarity rankings. More importantly, LSH operates in a data-independent manner and does not alter the underlying embedding space to enhance neighborhood preservation. As a result, while effective for coarse retrieval tasks, it lacks the ability to adaptively reshape embeddings to better retain k -NN structures in lower dimensions [31, 52], limiting its utility in scenarios demanding high-fidelity local ordering.

Graph-based indexing methods, such as Hierarchical Navigable Small World (HNSW)[32] and Navigating Spreading-out Graph (NSG)[15], construct sparse proximity graphs where each node links to its approximate neighbors. These methods enable extremely fast ANN retrieval with logarithmic search time. However, they operate

on fixed input embeddings and do not inherently perform dimensionality reduction, leaving the preservation of neighbor structure to the quality of the input vectors.

Some recent VLDB surveys [38, 50] emphasize the trade-offs among query speed, accuracy, and memory footprint in ANN systems. Emerging research [51, 52, 54] has explored index structure refinements for efficiency, yet they stop short of integrating dimensionality-aware neighborhood preservation strategies.

5.3 Neighbor- and Order-Preserving Dimensionality Reduction

Efforts to directly preserve nearest-neighbor or similarity order under DR are more recent and limited.

Order-preserving DR (OPDR) Evaluation [17] introduces a framework to analyze how DR affects similarity ranking among data points. By examining the functional relationship between target dimensionality and factors like variance retention or neighborhood distortion, OPDR enables systematic evaluation and design of dimensionality reduction techniques that better preserve neighborhood ordering.

Similarity Order Preserving Discriminant Analysis (SOPDA) [21] is a supervised DR method that uses class label information to enforce a similarity hierarchy: samples within the same class are embedded closer together in a manner that reflects their original similarity rankings. Although effective for classification tasks, SOPDA’s reliance on labeled data limits its applicability in unsupervised contexts like general-purpose ANN search.

Order-Preserving Hashing [49] addresses the preservation of similarity rankings in the binary hash space. It aims to maintain relative distances in the original space after hashing, facilitating ranked retrieval in hash-based indexing systems. Nevertheless, it outputs discrete binary codes and cannot be directly applied in scenarios requiring real-valued embeddings or differentiable mappings.

Earlier methods such as **dominance analysis in biomedical statistics** [29] implicitly used order-preserving principles to analyze time-series curves. However, they were domain-specific and not intended as general DR techniques.

Recent **contrastive learning approaches** [11, 19] learn embeddings that maintain semantic or local structure by contrasting positive and negative sample pairs. These methods often yield neighborhood-preserving features, albeit indirectly and at a high computational cost. Moreover, they require supervised signals or complex augmentations, posing challenges for large-scale, unsupervised retrieval tasks.

Graph sparsification techniques [27] and **all-range k -NN graphs** [54] complement dimensionality reduction (DR) by focusing on compact yet accurate representations of neighborhood structure in graph form. These methods aim to reduce redundancy in dense similarity graphs, enabling faster search and lower memory usage while preserving essential connectivity. In particular, all-range k -NN graphs extend conventional k -NN graphs by retaining top neighbors across a wide range of distances, improving global navigation without losing local fidelity. However, these techniques operate exclusively within the discrete graph domain and are typically applied post hoc to fixed vector embeddings. They do not modify or learn new low-dimensional representations of the input data, and thus cannot replace DR methods that seek to reshape continuous vector spaces in a way that preserves approximate nearest neighbor (ANN) relationships. As such, while valuable for graph-based indexing and retrieval, they are orthogonal to embedding-based dimensionality reduction approaches.

6 CONCLUSION AND FUTURE WORK

We presented MPAD, an unsupervised dimension-reduction framework that explicitly preserves local neighborhood structure for nearest-neighbor retrieval. Unlike conventional DR methods such as PCA and UMAP—which prioritize global variance or manifold embedding—MPAD promotes margin-based separation of true k -NNs from non-neighbors, ensuring that fine-grained geometric relationships remain intact. This design aligns with the practical demands of high-dimensional vector search, where preserving top- k neighbor consistency is often more critical than capturing broad data variance. Through extensive evaluations on diverse real-world datasets (text, speech, human health, and biological gene-expression profiles), MPAD demonstrates consistent gains in k -NN recall when

compared to standard DR techniques. In addition, our ablation studies show that MPAD’s performance is robust to moderate variations in its primary parameters, enabling smooth deployment across different domains without elaborate tuning. Moreover, the algorithm’s soft orthogonality constraint and margin-based formulation help it avoid degenerate projections while still achieving strong reduction ratios. Together, these results affirm MPAD’s effectiveness for retrieval-centric applications and highlight its ability to preserve semantically relevant neighborhoods in reduced-dimensional spaces. Potential directions for future work include investigating stochastic variants of MPAD tailored to very large datasets, exploring adaptive parameter schedules to further automate the projection process, and integrating MPAD into existing approximate nearest neighbor search pipelines for even more efficient retrieval.

REFERENCES

- [1] Dimitris Achlioptas. 2003. Database-friendly random projections: Johnson-Lindenstrauss with binary coins. *J. Comput. System Sci.* 66, 4 (2003), 671–687.
- [2] Karl Pearson and. 1901. LIII. On lines and planes of closest fit to systems of points in space. *The London, Edinburgh, and Dublin Philosophical Magazine and Journal of Science* 2, 11 (1901), 559–572. <https://doi.org/10.1080/14786440109462720> arXiv:<https://doi.org/10.1080/14786440109462720>
- [3] Alexandr Andoni, Piotr Indyk, and Ilya Razenshteyn. 2018. Approximate Nearest Neighbor Search in High Dimensions. *arXiv preprint arXiv:1806.09823* (2018).
- [4] Farzana Anowar, Samira Sadaoui, and Bassant Selim. 2021. Conceptual and empirical comparison of dimensionality reduction algorithms (pca, kpca, lda, mds, svd, lle, isomap, le, ica, t-sne). *Computer Science Review* 40 (2021), 100378.
- [5] Martin Aumüller, Erik Bernhardsson, and Alexander Faithfull. 2020. ANN-Benchmarks: A Benchmarking Tool for Approximate Nearest Neighbor Algorithms. *Information Systems* 87 (2020), 101374.
- [6] Mukund Balasubramanian and Eric L. Schwartz. 2002. The Isomap Algorithm and Topological Stability. *Science* 295, 5552 (2002), 7–7. <https://doi.org/10.1126/science.295.5552.7a> arXiv:<https://www.science.org/doi/pdf/10.1126/science.295.5552.7a>
- [7] Ella Bingham and Heikki Mannila. 2001. Random projection in dimensionality reduction: applications to image and text data. In *Proceedings of the seventh ACM SIGKDD international conference on Knowledge discovery and data mining*. 245–250.
- [8] Piotr Bojanowski, Edouard Grave, Armand Joulin, and Tomas Mikolov. 2016. Enriching Word Vectors with Subword Information. *arXiv preprint arXiv:1607.04606* (2016).
- [9] Emmanuel J Candès, Xiaodong Li, Yi Ma, and John Wright. 2011. Robust principal component analysis? *Journal of the ACM (JACM)* 58, 3 (2011), 1–37.
- [10] Huazhou Chen, Qi-Qing Song, Kai Shi, and Zhen Jia. 2015. [Multidimensional Scaling Linear Regression Applied to FTIR Spectral Quantitative Analysis of Clinical Parameters of Human Blood Serum]. *Guang pu xue yu guang pu fen xi = Guang pu* 35 (04 2015), 914–8. [https://doi.org/10.3964/j.issn.1000-0593\(2015\)04-0914-05](https://doi.org/10.3964/j.issn.1000-0593(2015)04-0914-05)
- [11] Ting Chen, Simon Kornblith, Mohammad Norouzi, and Geoffrey Hinton. 2020. A Simple Framework for Contrastive Learning of Visual Representations. In *Proceedings of the 37th International Conference on Machine Learning (ICML)*. 1597–1607.
- [12] Ron Cole and Mark Fandy. 1991. ISOLET. UCI Machine Learning Repository. DOI: <https://doi.org/10.24432/C51G69>.
- [13] Mayur Datar, Nicole Immorlica, Piotr Indyk, and Vahab Mirrokni. 2004. Locality-Sensitive Hashing Scheme Based on p -Stable Distributions. In *Proceedings of the 20th Annual Symposium on Computational Geometry (SoCG)*. 253–262.
- [14] Peter Frankl and Hiroshi Maehara. 1988. The Johnson-Lindenstrauss lemma and the sphericity of some graphs. *Journal of Combinatorial Theory, Series B* 44, 3 (1988), 355–362.
- [15] Cong Fu, Changxu Wang, and Deng Cai. 2017. Fast Approximate Nearest Neighbor Search With Navigating Spreading-out Graphs. *CoRR* abs/1707.00143 (2017). arXiv:1707.00143 <http://arxiv.org/abs/1707.00143>
- [16] Aristides Gionis, Piotr Indyk, and Rajeev Motwani. 1999. Similarity Search in High Dimensions via Hashing. In *Proceedings of the 25th International Conference on Very Large Data Bases (VLDB)*. 518–529.
- [17] Chengyu Gong, Gefei Shen, Luanzheng Guo, Nathan Tallent, and Dongfang Zhao. 2024. OPDR: Order-Preserving Dimension Reduction for Semantic Embedding of Multimodal Scientific Data. arXiv:2408.10264 [cs.LG] <https://arxiv.org/abs/2408.10264>
- [18] Isabelle Guyon, Steve Gunn, Asa Ben-Hur, and Gideon Dror. 2004. Arcene. UCI Machine Learning Repository. DOI: <https://doi.org/10.24432/C58P55>.

- [19] Raia Hadsell, Sumit Chopra, and Yann LeCun. 2006. Dimensionality Reduction by Learning an Invariant Mapping. In *Proceedings of the IEEE Conference on Computer Vision and Pattern Recognition (CVPR)*. 1735–1742.
- [20] Trevor Hastie and Werner Stuetzle and. 1989. Principal Curves. *J. Amer. Statist. Assoc.* 84, 406 (1989), 502–516. <https://doi.org/10.1080/01621459.1989.10478797> arXiv:<https://www.tandfonline.com/doi/pdf/10.1080/01621459.1989.10478797>
- [21] HaoShuang Hu, Da-Zheng Feng, and Qing-Yan Chen. 2021. A novel dimensionality reduction method: Similarity order preserving discriminant analysis. *Signal Processing* 182 (2021), 107933. <https://doi.org/10.1016/j.sigpro.2020.107933>
- [22] Piotr Indyk and Rajeew Motwani. 1998. Approximate Nearest Neighbors: Towards Removing the Curse of Dimensionality. In *Proceedings of the 30th ACM Symposium on Theory of Computing (STOC)*. 604–613.
- [23] Weikuan Jia, Meili Sun, Jian Lian, and Sujuan Hou. 2022. Feature dimensionality reduction: a review. *Complex & Intelligent Systems* 8, 3 (2022), 2663–2693.
- [24] Ian Jolliffe. 2002. *Principal Component Analysis*. Springer.
- [25] Armand Joulin, Edouard Grave, Piotr Bojanowski, Matthijs Douze, Herve Jégou, and Tomas Mikolov. 2016. FastText.zip: Compressing text classification models. *arXiv preprint arXiv:1612.03651* (2016).
- [26] Armand Joulin, Edouard Grave, Piotr Bojanowski, and Tomas Mikolov. 2016. Bag of Tricks for Efficient Text Classification. *arXiv preprint arXiv:1607.01759* (2016).
- [27] Abd Errahmane Kiouche, Julien Baste, Mohammed Haddad, Hamida Seba, and Angela Bonifati. 2024. Neighborhood-Preserving Graph Sparsification. *Proc. VLDB Endow.* 17, 13 (2024), 4853–4866. <https://www.vldb.org/pvldb/vol17/p4853-seba.pdf>
- [28] Oliver Kramer. 2013. *K-Nearest Neighbors*. Springer Berlin Heidelberg, Berlin, Heidelberg, 13–23. https://doi.org/10.1007/978-3-642-38652-7_2
- [29] Sang Han Lee, Johan Lim, Marina Vannucci, Eva Petkova, Maurice Preter, and Donald F. Klein. 2008. Order-Preserving Dimension Reduction Procedure for the Dominance of Two Mean Curves with Application to Tidal Volume Curves. *Biometrics* 64, 3 (01 2008), 931–939. <https://doi.org/10.1111/j.1541-0420.2007.00959.x> arXiv:https://academic.oup.com/biometrics/article-pdf/64/3/931/52729767/biometrics_64_3_931.pdf
- [30] Haiping Lu, Konstantinos N Plataniotis, and Anastasios N Venetsanopoulos. 2008. MPCA: Multilinear principal component analysis of tensor objects. *IEEE transactions on Neural Networks* 19, 1 (2008), 18–39.
- [31] Qin Lv, William Josephson, Zhe Wang, Moses Charikar, and Kai Li. 2007. Multi-Probe LSH: Efficient Indexing for High-Dimensional Similarity Search. In *Proceedings of the 33rd International Conference on Very Large Data Bases (VLDB)*. 950–961.
- [32] Yu A Malkov and D A Yashunin. 2018. Efficient and robust approximate nearest neighbor search using Hierarchical Navigable Small World graphs. *IEEE transactions on pattern analysis and machine intelligence* 42, 4 (2018), 824–836.
- [33] Sanparith Marukatat. 2023. Tutorial on PCA and approximate PCA and approximate kernel PCA. *Artificial Intelligence Review* 56, 6 (2023), 5445–5477.
- [34] Jiří Matoušek. 2008. On variants of the Johnson–Lindenstrauss lemma. *Random Structures & Algorithms* 33, 2 (2008), 142–156.
- [35] Leland McInnes, John Healy, and James Melville. 2018. UMAP: Uniform manifold approximation and projection for dimension reduction. *arXiv preprint arXiv:1802.03426* (2018).
- [36] A. Mead. 1992. Review of the Development of Multidimensional Scaling Methods. *Journal of the Royal Statistical Society. Series D (The Statistician)* 41, 1 (1992), 27–39. <http://www.jstor.org/stable/2348634>
- [37] Marius Muja and David G. Lowe. 2014. Scalable Nearest Neighbor Algorithms for High Dimensional Data. *IEEE Transactions on Pattern Analysis and Machine Intelligence* 36, 11 (2014), 2227–2240.
- [38] Jianbin Qin, Wei Wang, Chuan Xiao, and Ying Zhang. 2020. Similarity Query Processing for High-Dimensional Data. *Proc. VLDB Endow.* 13, 12 (2020), 3437–3440. <https://doi.org/10.14778/3415478.3415564>
- [39] Sam T. Roweis and Lawrence K. Saul. 2000. Nonlinear Dimensionality Reduction by Locally Linear Embedding. *Science* 290, 5500 (2000), 2323–2326. <https://doi.org/10.1126/science.290.5500.2323> arXiv:<https://www.science.org/doi/pdf/10.1126/science.290.5500.2323>
- [40] Rahul Satija, Jeffrey A Farrell, David Gennert, Alexander F Schier, and Aviv Regev. 2015. Spatial reconstruction of single-cell gene expression data. *Nature Biotechnology* 33, 5 (2015), 495–502.
- [41] Lawrence K Saul and Sam T Roweis. 2000. An introduction to locally linear embedding. *unpublished. Available at: http://www.cs.toronto.edu/~roweis/llc/publications.html* (2000).
- [42] Bernhard Schölkopf, Alexander Smola, and Klaus-Robert Müller. 1998. Nonlinear Component Analysis as a Kernel Eigenvalue Problem. *Neural Computation* 10, 5 (07 1998), 1299–1319. <https://doi.org/10.1162/089976698300017467> arXiv:<https://direct.mit.edu/neco/article-pdf/10/5/1299/813905/089976698300017467.pdf>
- [43] Kirill Simonov, Fedor Fomin, Petr Golovach, and Fahad Panolan. 2019. Refined Complexity of PCA with Outliers. In *Proceedings of the 36th International Conference on Machine Learning (Proceedings of Machine Learning Research)*, Kamalika Chaudhuri and Ruslan Salakhutdinov (Eds.), Vol. 97. PMLR, 5818–5826. <https://proceedings.mlr.press/v97/simonov19a.html>
- [44] Joshua B. Tenenbaum, Vin de Silva, and John C. Langford. 2000. A Global Geometric Framework for Nonlinear Dimensionality Reduction. *Science* 290, 5500 (2000), 2319–2323. <https://doi.org/10.1126/science.290.5500.2319> arXiv:<https://www.science.org/doi/pdf/10.1126/science.290.5500.2319>
- [45] Michael W. Trosset and Carey E. Priebe. 2008. The out-of-sample problem for classical multidimensional scaling. *Computational Statistics & Data Analysis* 52, 10 (2008), 4635–4642. <https://doi.org/10.1016/j.csda.2008.02.031>
- [46] Laurens van der Maaten and Geoffrey Hinton. 2008. Visualizing data using t-SNE. *Journal of machine learning research* 9, Nov (2008), 2579–2605.
- [47] Laurens Van Der Maaten, Eric O Postma, H Jaap Van Den Herik, et al. 2009. Dimensionality reduction: A comparative review. *Journal of machine learning research* 10, 66-71 (2009), 13.
- [48] Santosh S Vempala. 2005. *The random projection method*. Vol. 65. American Mathematical Soc.
- [49] Jianfeng Wang, Jingdong Wang, Nenghai Yu, and Shipeng Li. 2013. Order preserving hashing for approximate nearest neighbor search. In *Proceedings of the 21st ACM International Conference on Multimedia (Barcelona, Spain) (MM '13)*. Association for Computing Machinery, New York, NY, USA, 133–142. <https://doi.org/10.1145/2502081.2502100>
- [50] Mengzhao Wang, Xiaoliang Xu, Qiang Yue, and Yuxiang Wang. 2021. A Comprehensive Survey and Experimental Comparison of Graph-Based Approximate Nearest Neighbor Search. *Proc. VLDB Endow.* 14, 11 (2021), 1964–1978. <https://doi.org/10.14778/3476249.3476255>
- [51] Xi Zhao, Yao Tian, Kai Huang, Bolong Zheng, and Xiaofang Zhou. 2023. Towards Efficient Index Construction and Approximate Nearest Neighbor Search in High-Dimensional Spaces. *Proc. VLDB Endow.* 16, 8 (2023), 1979–1991. <https://doi.org/10.14778/3594512.3594527>
- [52] Bolong Zheng, Xi Zhao, Lianggui Weng, Nguyen Quoc Viet Hung, Hang Liu, and Christian S. Jensen. 2020. PM-LSH: A Fast and Accurate LSH Framework for High-Dimensional Approximate NN Search. *Proc. VLDB Endow.* 13, 5 (2020), 643–655. <https://doi.org/10.14778/3377369.3377374>
- [53] Hui Zou, Trevor Hastie, and Robert Tibshirani. 2006. Sparse principal component analysis. *Journal of computational and graphical statistics* 15, 2 (2006), 265–286.
- [54] Chaoji Zuo and Dong Deng. 2023. ARKGraph: All-Range Approximate K-Nearest-Neighbor Graph. *Proc. VLDB Endow.* 16, 10 (2023), 2645–2658. <https://doi.org/10.14778/3603581.3603601>